

***n-p* Charge-Exchange Scattering from 60 to 300 GeV/c\***

H. R. Barton, Jr.,† N. W. Reay, K. Reibel, M. Shaevitz,‡ and N. R. Stanton  
*The Ohio State University, Columbus, Ohio 43210*

and

M. A. Abolins, P. Brindza,† J. A. J. Matthews,§ and R. Sidwell  
*Michigan State University, East Lansing, Michigan 48823*

and

K. W. Edwards and G. Luxton||  
*Carleton University, Ottawa, Ontario K1S 5B6, Canada*

and

P. Kitching  
*University of Alberta, Edmonton, Alberta, Canada*  
 (Received 4 October 1976)

We have measured the neutron-proton charge-exchange differential cross section in the momentum interval 60 to 300 GeV/c, with squared four-momentum transfers 0.002 to 0.8 (GeV/c)<sup>2</sup>. Independent of incident momentum, the data are characterized by a sharp forward peak of width 0.02 (GeV/c)<sup>2</sup>, followed by a shoulder and gentler falloff at higher momentum transfers.

The differential cross section for neutron-proton charge-exchange scattering below 60 GeV/c is characterized by a "pion-exchange" peak of width  $M_\pi^2 \sim 0.02$  (GeV/c)<sup>2</sup> at small squared momentum transfers ( $t$ ), followed by a much gentler slope at higher  $|t|$ .<sup>1</sup> The cross section has a  $P_{\text{lab}}^{-n}$  dependence on incident momentum, where  $n$  is independent of  $t$  but decreases from 2.0 for momenta below 10 GeV/c to 1.5 near 60 GeV/c. Whether the cross-section shape remains invariant and  $n$  continues to fall above 60 GeV/c is important to many models of strong interactions. Further, the  $n$ - $p$  charge-exchange cross section extrapolated to  $|t|=0$  provides a bound on the difference between  $n$ - $p$  and  $p$ - $p$  total cross sections.

Our data sample of 25000 events was obtained in the momentum interval 60 to 300 GeV/c and squared momentum transfers 0.002 to 0.8 (GeV/c)<sup>2</sup> using the apparatus shown in Fig. 1. The

Fermilab M3 neutral beam was produced at  $\frac{3}{4}$  mrad from the interactions of 300-GeV/c protons with a beryllium target. Passage through a series of collimators, sweeping magnets, and 3 in. of lead filtering removed charged particles, beam halo, and  $\gamma$ -ray contamination; the  $K_L^0$  flux in the beam was negligible above 60 GeV.<sup>2</sup> The resulting neutron spectral shape, as shown in Fig. 2, was taken as an average of that determined by the Northwestern-Rochester-Stanford Linear Accelerator Center collaboration using Coulomb excitation of  $\Delta(1238)$ ,<sup>3</sup> and by Murthy *et al.* (and by us) using the Michigan neutron calorimeter.<sup>2</sup> The total flux was typically  $5 \times 10^5$  neutrons/pulse.

The target consisted of two sections of liquid hydrogen each 4 in. long, separated by a thin scintillator tagging events occurring in the upstream half.

Recoil neutrons from the liquid hydrogen target were detected in two banks of neutron counters,

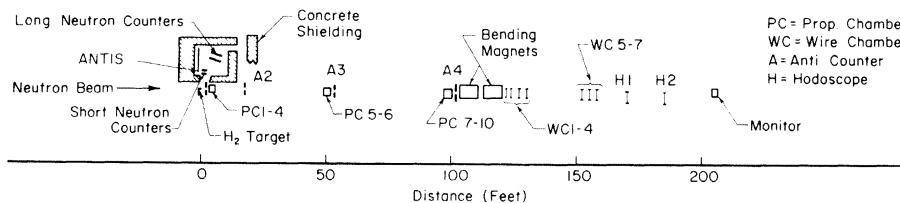


FIG. 1. Experimental layout. The upstream anti counter is not shown.

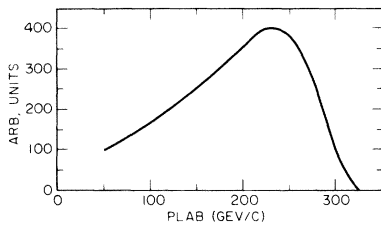


FIG. 2. Relative incident neutron-beam intensity as a function of incident momentum.

each containing fourteen counters mounted horizontally. The wide-angle bank contained 3-in.  $\times$  6-in.  $\times$  25-in. "short" plastic scintillator counters placed radially about 6 ft from the target and set with 0.1-MeV electron equivalent thresholds for detection of slow recoils. The more forward-angle bank contained 4-in.  $\times$  12-in.  $\times$  60-in. "long" counters placed typically 12 ft from the target and had 1.0-MeV thresholds to detect higher energy neutrons. The magnitude of the neutron vector momentum was measured by time of flight, its azimuth by recording which counter fired, and the polar angle by performing timing between the ends of each counter. Timing and spatial resolution were consistent with the measurements presented in a previous paper.<sup>4</sup>

The forward-going protons were detected in a magnetic spectrometer containing proportional wire chambers in the upstream leg and magnetostrictive spark chambers in the downstream leg. Sufficient chambers were used to insure a spectrometer efficiency in excess of 99% for charge-exchange events.

Non-charge-exchange events were suppressed by anti counters surrounding all but the downstream side of the target, by a series of lead-scintillator aperture anti counters placed throughout the upstream leg of the spectrometer, and by a trigger requiring a single minimum-ionizing pulse height in the scintillation counter just downstream of the target. Non-target-associated particles triggering the neutron counters were suppressed by extensive concrete shielding and by an upstream wall of anti counters.

The neutron counter thresholds and efficiencies were determined by methods described elsewhere.<sup>4-6</sup> Cross sections from each of the counters of a given bank agreed within statistics, and changed less than 10% when thresholds were raised a factor of 2.4 and efficiencies lowered correspondingly. In the region of overlap between 0.04 and 0.08 (GeV/c)<sup>2</sup>, cross sections from the two types of counters agreed to better than 8%

and were statistically averaged.

In off-line analysis, approximately one million triggers yielded 500 000 tracks passing clearly through the entire system. Extraction of three-constraint elastic events from background relied mainly on coplanarity and  $P_{\perp}$  momentum balance between neutron and proton arms, and hence alignment of the proton arm to  $10^{-5}$  rad using straight-through muons was essential. A full kinematic fit was made using measured neutron and proton vector momenta; if more than one neutron counter fired, all possibilities were tried and the combination kept with lowest  $\chi^2$ .

Fits to the  $\chi^2$  distribution were then performed to estimate the background contamination in the final data sample of 25 000 events. Such back-

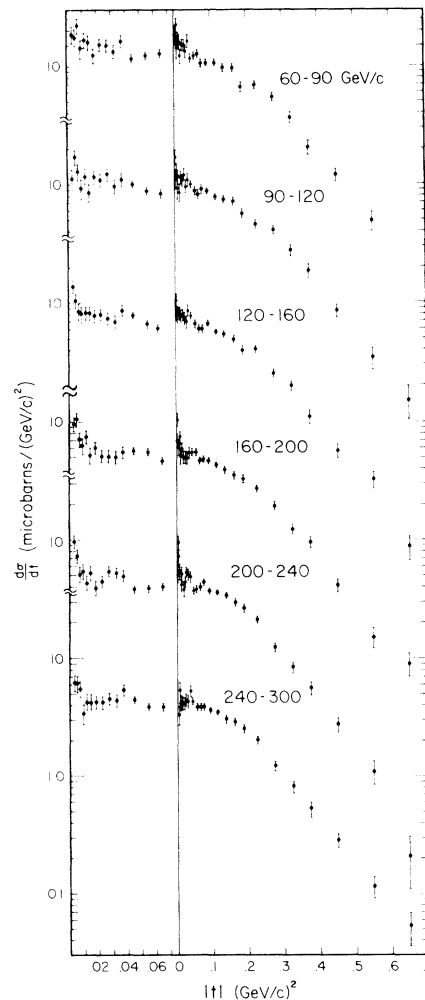


FIG. 3.  $n$ - $p$  charge-exchange absolute cross sections. The data are shown using the binning of Table I, and the errors shown are statistical only. Small-momentum-transfer data are shown in an expanded  $|t|$  scale for ease in viewing.

TABLE I.  $n$ - $p$  charge-exchange differential cross section presented as a function of momentum transfer in six bins of incident momentum. The  $\pm 6\%$  point-to-point uncertainty in efficiency and the overall  $\pm 15\%$  uncertainty in absolute normalization are not included.

$t$ [(GeV/c) <sup>2</sup> ]	INCIDENT MOMENTUM (GeV/c)					
	60-90	90-120	120-160	160-200	200-240	240-300
.0030	18.01 ± 3.04	10.94 ± 2.10	13.76 ± 1.79	9.34 ± 1.28	9.67 ± 1.17	6.14 ± .93
.0050	18.41 ± 2.98	17.55 ± 2.58	10.54 ± 1.52	10.45 ± 1.31	7.49 ± 1.00	6.32 ± .92
.0070	21.95 ± 3.23	13.15 ± 2.22	8.43 ± 1.35	7.19 ± 1.08	5.01 ± .81	5.43 ± .84
.0090	14.00 ± 2.55	9.19 ± 1.87	8.04 ± 1.30	6.23 ± .99	5.54 ± .84	3.62 ± .68
.0115	16.55 ± 2.29	12.53 ± 1.77	8.22 ± 1.08	7.52 ± .90	4.39 ± .62	4.24 ± .50
.0145	16.01 ± 2.28	8.74 ± 1.50	8.44 ± 1.11	5.25 ± .76	5.23 ± .68	4.26 ± .62
.0180	12.85 ± 1.80	12.11 ± 1.55	7.88 ± .94	5.95 ± .71	4.11 ± .53	4.33 ± .55
.0225	15.08 ± 1.81	11.19 ± 1.38	8.12 ± .89	5.23 ± .62	4.47 ± .51	4.24 ± .50
.0275	15.43 ± 1.87	12.15 ± 1.47	7.51 ± .87	5.05 ± .62	5.39 ± .58	4.66 ± .54
.0325	13.41 ± 1.76	9.83 ± 1.33	7.02 ± .85	4.98 ± .62	5.43 ± .58	4.36 ± .52
.0375	16.32 ± 1.99	10.93 ± 1.44	8.72 ± .98	5.50 ± .67	4.91 ± .57	5.34 ± .60
.0450	11.83 ± .89	10.12 ± .73	7.89 ± .49	5.65 ± .36	3.80 ± .26	4.41 ± .28
.0550	12.34 ± .92	8.86 ± .69	6.81 ± .46	5.48 ± .36	4.80 ± .30	3.87 ± .27
.0650	12.84 ± .95	8.43 ± .68	6.20 ± .44	4.66 ± .33	4.01 ± .27	3.80 ± .27
.0750	10.71 ± .87	9.08 ± .71	5.97 ± .44	4.74 ± .34	4.45 ± .29	3.86 ± .27
.0900	10.70 ± .63	8.79 ± .51	6.79 ± .34	4.72 ± .24	3.70 ± .19	3.64 ± .19
.1125	10.68 ± .60	7.90 ± .45	5.69 ± .29	4.31 ± .22	3.61 ± .18	3.50 ± .18
.1375	9.73 ± .76	7.56 ± .59	5.11 ± .38	3.68 ± .28	3.40 ± .23	3.06 ± .22
.1625	9.84 ± .80	7.23 ± .61	4.97 ± .38	3.52 ± .28	2.95 ± .23	2.91 ± .23
.1875	6.69 ± .67	5.81 ± .56	3.97 ± .35	3.28 ± .27	2.70 ± .22	2.54 ± .22
.2250	7.04 ± .50	4.72 ± .36	4.08 ± .25	2.74 ± .18	2.12 ± .14	2.04 ± .14
.2750	5.55 ± .46	4.07 ± .35	2.55 ± .21	1.94 ± .15	1.22 ± .11	1.23 ± .11
.3250	3.70 ± .38	2.79 ± .29	2.00 ± .19	1.25 ± .13	.84 ± .09	.81 ± .09
.3750	2.06 ± .28	1.88 ± .24	1.08 ± .14	.95 ± .11	.57 ± .08	.52 ± .07
.4500	1.20 ± .15	.84 ± .11	.54 ± .07	.41 ± .05	.28 ± .04	.28 ± .03
.5500	.49 ± .09	.34 ± .07	.31 ± .05	.14 ± .03	.11 ± .01	.11 ± .02
.6500	.16 ± .05	.14 ± .04	.08 ± .02	.08 ± .02	.02 ± .01	.05 ± .01
.7500	.08 ± .03	.08 ± .03	.03 ± .01	.02 ± .01	.004 ± .004	.004 ± .004
	75	105	140	180	220	260
	AVERAGE MOMENTUM (GeV/c)					

grounds were typically 5% for the large neutron counters, rising to 12% at the highest momentum transfers, and 10% for the small neutron counters, rising to 27% in the smallest momentum-transfer bin. As target-empty backgrounds were always less than 2%, most of these backgrounds arose from inelastic scattering within the hydrogen target. Uncertainties in background subtraction always were less than  $\frac{1}{5}$  of the subtraction.

Corrections were applied for anti overkill [typically  $(10 \pm 1)\%$ ], losses from the proton pulse-height cut  $(7 \pm 1)\%$ , absorption (largely in the target) of the recoil neutron before reaching the neutron counters, 37% for the smallest momentum transfer bin to 2% for the highest. It is estimated that the absorption corrections were known to 10% of their absolute value. Proton absorption losses were compensated by losses in the neutron beam before it arrived at the downstream beam monitor. A small correction (1 to 2%) was applied for events in which the time of flight was stopped by randoms in the neutron counter, and a 2% correction was applied for losses due to the  $\chi^2$  cut in the kinematic fitting.

The data are shown in Fig. 3 and Table I. The errors shown are statistical only and include neither the  $\pm 6\%$  point-to-point uncertainty in neutron counter efficiency nor the  $\pm 15\%$  error in ab-

solute normalization. The latter error was derived equally from the differences of up to 10% between the various methods of measuring the beam spectrum, and from uncertainties in calibration and stability of the downstream beam monitor. Specifically, if the various methods of momentum-dependent beam normalization are normalized to the total flux, good agreement is achieved everywhere but in the momentum region 60–80 GeV/c, where discrepancies of up to 10% are noted. The smallest momentum-transfer bin has an additional  $\pm 10\%$  error due to uncertainties in thresholds and absorption corrections.

A detailed discussion of the data is presented in a companion paper.

We are indebted to J. Fitch, A. Raffler, D. Keithly, and D. O'Hara for the design and construction of the mechanical hardware, C. Rush and H. Coombes for design and implementation of the electronics, and B. Dodge, K. Safinya, E. Lulofs, R. Kammerud, and D. Cardimona, who participated in various aspects of the experiment. We wish to thank the University of Michigan group for the use of their calorimeter, and to thank the staff of Fermilab, who gave us help at every juncture.

\*Work supported in part by the U. S. Energy Research

and Development Administration, the National Science Foundation, and the National Research Council, Canada.

†Present address: Fermilab, Batavia, Ill. 60510.

‡Present address: California Institute of Technology, Pasadena, Calif. 91109.

§Present address: Johns Hopkins University, Baltimore, Md. 21218.

¶Present address: Department of Radiology, Stanford University, Stanford, Calif. 94305.

<sup>1</sup>E. L. Miller *et al.*, Phys. Rev. Lett. **26**, 984 (1971); J. Engler *et al.*, Phys. Lett. **34B**, 528 (1971); M. N.

Kreisler *et al.*, Nucl. Phys. **B84**, 3 (1975); V. Böhmer *et al.*, Nucl. Phys. **B110**, 205 (1976); A. Babaev *et al.*, Nucl. Phys. **B110**, 189 (1976).

<sup>2</sup>P. V. R. Murthy *et al.*, Nucl. Phys. **B92**, 269 (1975).

<sup>3</sup>R. Ruchti, Northwestern University, private communication.

<sup>4</sup>M. Elfield *et al.*, Nucl. Instrum. Methods **100**, 237 (1972).

<sup>5</sup>R. M. Edelstein *et al.*, Nucl. Instrum. Methods **100**, 355 (1972).

<sup>6</sup>N. R. Stanton, Ohio State University Report No. COO-1545-92, February 1971 (unpublished).

## Some Features of $n$ - $p$ Charge-Exchange Scattering between 60 and 300 GeV/ $c$ \*

H. R. Barton, Jr.,† N. W. Reay, K. Reibel, M. Shaevitz,‡ and N. R. Stanton  
*The Ohio State University, Columbus, Ohio 43210*

and

M. A. Abolins, P. Brindza,† J. A. J. Matthews,§ and R. Sidwell  
*Michigan State University, East Lansing, Michigan 48823*

and

K. W. Edwards and G. Luxton||  
*Carleton University, Ottawa, Ontario K1S 5B6, Canada*

and

P. Kitching  
*University of Alberta, Edmonton, Alberta, Canada*  
(Received 4 October 1976)

We examine the dependence of the  $n$ - $p$  charge-exchange cross section on the squared four-momentum transfer and on the incident momentum, and include some comparisons with data from lower energies. Implications for the difference between  $n$ - $p$  and  $p$ - $p$  total cross sections are presented.

In the previous Letter we presented the results of a new measurement of the  $n$ - $p$  charge exchange differential cross section covering incident momenta from 60 to 300 GeV/ $c$  and squared four-momentum transfers ( $t$ ) from 0.002 to 0.8 (GeV/ $c$ )<sup>2</sup>.<sup>1</sup> We present here an analysis of the data in which we examine the energy dependence of this reaction, and use the  $t=0$  differential cross-section points to set bounds on the difference of the  $n$ - $p$  and  $p$ - $p$  total cross sections.

All  $n$ - $p$  charge-exchange cross sections<sup>1-5</sup> above 3 GeV/ $c$  may be fitted acceptably for  $|t|$  less than 0.07 (GeV/ $c$ )<sup>2</sup> by the form

$$\frac{d\sigma}{dt} = A \left( \frac{m_\pi^4}{(|t| + m_\pi^2)^2} \right) + B. \quad (1)$$

The phenomenological expression is motivated by

models incorporating pion exchange with absorption<sup>6</sup> and is useful in displaying the energy dependence of the size of the "pion" peak relative to the background. At  $t=0$ , the differential cross section is the sum of the "pion" contribution whose coefficient is  $A$  and the sum of all other contributions given by  $B$ . The ratio  $A/B$  is a measure of the relative size of the forward peak independent of normalization. We have fitted our data and those of others to expression (1) over a range of  $|t|$  in the forward direction. The fits appear to be stable within errors for starting points ranging from 0.002 to 0.008 (GeV/ $c$ )<sup>2</sup> and end points from 0.05 to 0.07 (GeV/ $c$ )<sup>2</sup>. In Fig. 1 are plotted the results of fits to our data for the region  $0.002 < |t| < 0.06$  (GeV/ $c$ )<sup>2</sup>, and in Table I we summarize our data as well as those of others.